High-Efficiency Polycrystalline Thin Film Tandem Solar Cells

ARTICLE *in* JOURNAL OF PHYSICAL CHEMISTRY LETTERS · JUNE 2015

Impact Factor: 7.46 · DOI: 10.1021/acs.jpclett.5b01108

11 AUTHORS, INCLUDING:

Lukas Kranz

29 PUBLICATIONS **650** CITATIONS

SEE PROFILE

Antonio Abate

École Polytechnique Fédérale de Lausanne

58 PUBLICATIONS **1,518** CITATIONS

SEE PROFILE

Fan Fu

Empa - Swiss Federal Laboratories for Materi…

8 PUBLICATIONS **52** CITATIONS

SEE PROFILE

Patrick Reinhard

Empa - Swiss Federal Laboratories for Materi…

23 PUBLICATIONS **293** CITATIONS

SEE PROFILE

THE JOURNAL OF PHYSICAL CHEMISTRY Letters

Letter

pubs.acs.org/JPCL

High-Efficiency Polycrystalline Thin Film Tandem Solar Cells

Lukas Kranz,[†,⊥] Antonio Abate,[‡] Thomas Feurer,[†] Fan Fu,[†] Enrico Avancini,[†] Johannes Löckinger,[†] Patrick Reinhard,[†] Shaik M. Zakeeruddin,[‡,§] Michael Grätzel,*[,‡] Stephan Buecheler,*[,†] and Ayodhya N. Tiwari[†]

[†]Laboratory for Thin Films and Photovoltaics, Empa—Swiss Federal Laboratories for Materials Science and Technology, Ueberlandstrasse 129, 8600 Duebendorf, Switzerland

[‡]Laboratory for Photonics and Interfaces, Institute of Chemical Sciences and Engineering, École Polytechnique Fédérale de Lausanne, CH-1015-Lausanne, Switzerland

[§]Center of Excellence for Advanced Materials Research (CEAMR), King Abdulaziz University, Jeddah 22254, Saudi Arabia

Supporting Information

ABSTRACT: A promising way to enhance the efficiency of CIGS solar cells is by combining them with perovskite solar cells in tandem devices. However, so far, such tandem devices had limited efficiency due to challenges in developing NIR-transparent perovskite top cells, which allow photons with energy below the perovskite band gap to be transmitted to the bottom cell. Here, a process for the fabrication of NIR-transparent perovskite solar cells is presented, which enables power conversion efficiencies up to 12.1% combined with an average sub-band gap transmission of 71% for photons with wavelength between 800 and 1000 nm. The combination of a NIR-transparent perovskite top cell with a CIGS bottom cell enabled a tandem device with 19.5% efficiency, which is the highest reported efficiency for a polycrystalline thin film tandem solar cell. Future developments of perovskite/CIGS tandem devices are discussed and prospects for devices with efficiency toward and above 27% are given.

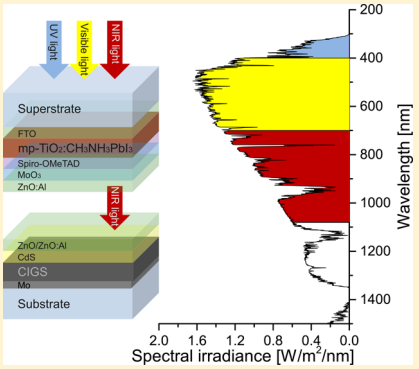

Cost of thin film photovoltaic (PV) modules is continuously decreasing and currently a major part of the cost of PV-generated electricity is caused by balance of system (BOS) costs.[1] A viable way to reduce BOS costs per W_P is by enhancing efficiency of the solar modules. Efficiency of PV devices can be improved by combining two solar cell technologies in a tandem structure,[2] where a larger band gap (∼1.5−1.8 eV) solar cell is stacked on a smaller band gap (∼0.9−1.2 eV) solar cell. The top cell converts high-energy photons with minimized thermalization loss and transmits the near-infrared (NIR) part of the solar spectrum into the bottom cell. The concept of tandem devices has been successfully applied in the field of III−V semiconductor single crystal solar cells, where power conversion efficiencies up to 31.1% have been achieved under 1 sun.[3] Also various types of low-cost thin film solar cells have been combined in tandem devices,[4−7] where the highest reported efficiency of 15.8% has been achieved with dye-sensitized/$Cu(In,Ga)Se_2$ (CIGS) tandem solar cells.[4,5]

Until recently, one of the major limitations for the realization of high performance polycrystalline thin film tandem devices has been the lack of a high-efficiency top cell with a band gap larger than 1.5 eV and low sub-band gap absorption. The recently introduced solar cells based on hybrid organic−inorganic perovskites, such as $CH_3NH_3PbI_3$, offer the possibility to overcome these limitations. Following the initial work by Kojima et al.,[8] unprecedented efficiency improvements have been achieved within only a few years.[9−13] The low sub-band gap absorption of $CH_3NH_3PbI_3$[14] as well as its band gap of ∼1.57 eV, which is further tunable up to ∼2.3 eV by replacement of iodine by bromine,[15] makes this material ideal for the application as a top cell in tandem devices.[16−21] One of the major challenges to experimentally realize perovskite-based tandem cells is the development of perovskite solar cells in which the metallic contact is replaced by a transparent contact, so that photons with energy below the perovskite band gap are transmitted to the bottom cell. Löper et al. presented a perovskite top cell with 6.2% efficiency, where the metallic electrode was replaced by a MoO_3/ITO contact, leading to a perovskite/c-Si tandem cell with 13.4% efficiency.[20] Bailie et al. used a Ag nanowire based hole collecting contact, leading to 18.6% and 17.0% efficient perovskite/CIGS and perovskite/c-Si tandem solar cells, respectively. These are very promising results; however, the process for the application of the Ag nanowires is complex and variability in the applied force can cause shorting as well as incomplete transfer, resulting in a spread of device efficiencies.[21] In this respect, a sputter-based process for the transparent top electrode would be advantageous.

Received: May 27, 2015
Accepted: June 22, 2015

DOI: 10.1021/acs.jpclett.5b01108
J. Phys. Chem. Lett. 2015, 6, 2676−2681

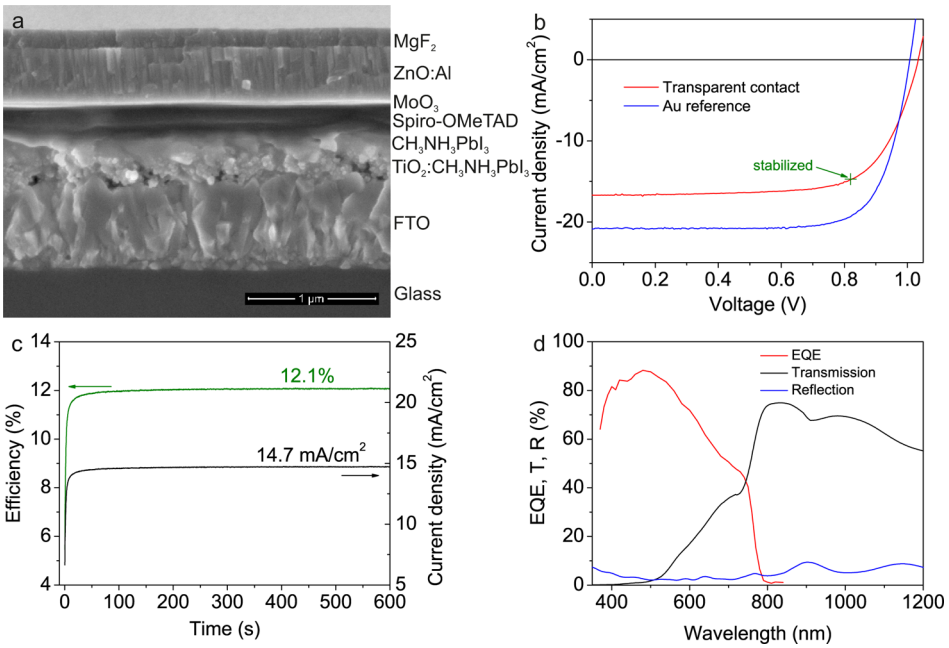

Figure 1. Characterization of NIR-transparent perovskite cells. (a) Cross-sectional SEM image of the cell; the compact TiO_2 layer is not visible. (b) $J-V$ characteristics of the best device. For comparison, the $J-V$ characteristics of the reference with Au electrode is shown. The corresponding PV parameters are listed in Table 1. Illumination intensity for the perovskite cell with transparent contact is 1000 W/m^2, whereas it is 984 W/m^2 for the reference cell with Au contact. (c) Steady-state current density measurement at maximum power point (820 mV) and corresponding steady-state efficiency of the best device. (d) EQE as well as total transmission and reflection measurements of the best device.

In this paper, we present a process for the fabrication of NIR-transparent perovskite solar cells with sputter deposited transparent top electrode, which enables up to 12.1% steady-state power conversion efficiency. By combining a NIR-transparent perovskite solar cell with a CIGS solar cell, we achieved a tandem solar cell efficiency of 19.5%. This is the highest reported efficiency for an all-thin film polycrystalline tandem solar cell.

Perovskite solar cells in superstrate configuration are processed from solution as detailed in the Supporting Information. The top electrode is made by a transparent layer stack to enable high NIR-transparency of the top cell. MoO_3 is deposited by vacuum evaporation on the hole extraction layer spiro-OMeTAD (2,2′,7,7′-tetrakis(*N*,*N*-di-*p*-methoxyphenylamine)-9,9′-spirobifluorene) followed by a sputtered ZnO:Al transparent conductive oxide (TCO) layer and a metallic grid. To minimize damage to the underlying layers during the TCO deposition a soft ZnO:Al sputter process is developed, which is described in the Supporting Information. The layer stack of the NIR-transparent perovskite cells is FTO/TiO_2/mp-TiO_2:$CH_3NH_3PbI_3$/$CH_3NH_3PbI_3$/spiro-OMeTAD/MoO_3/ZnO:Al/Ni-Al grid/MgF_2. A cross-sectional scanning electron microscope (SEM) image of a NIR-transparent perovskite cell is shown in Figure 1a.

Figure 1b displays the current density−voltage ($J-V$) characteristics of the best-performing NIR-transparent perovskite cell and of the nontransparent reference cell with Au top electrode. The corresponding PV parameters are summarized in Table 1.

The best NIR-transparent cell has an efficiency of 12.1% with a high open circuit voltage V_{OC} > 1 V and fill factor FF > 70%. Because perovskite solar cells can exhibit hysteresis effects,[22] we further present the steady-state efficiency as measured by maintaining the cell at a constant forward bias of 820 mV (Figure 1c). At 820 mV bias voltage, a steady-state current density of 14.7 mA/cm^2 and efficiency of 12.1% are measured, confirming the performance parameters deduced from $J-V$ characteristics. The V_{OC} of the best NIR-transparent cell is similar to the V_{OC} of the nontransparent cell, with even a small improvement by 26 mV in the NIR-transparent cell, similar to what was observed in a previous study by Bailie et al.[21] The FF is slightly reduced from 75.2% to 70.3% upon replacement of the Au layer with the transparent contact. The reduction is ascribed to a lower conductivity of the TCO compared to the metal contact. A significant difference between the PV parameters of the NIR-transparent and reference cell is observed in the short circuit current density (J_{SC}), which is 4.1 mA/cm^2 lower in the NIR-transparent cell. This difference is ascribed to incomplete absorption in the NIR-transparent cell in the wavelength region ~550−780 nm, which is confirmed by external quantum efficiency (EQE) measurements (Figure 1d). In the Au reference, the metallic contact leads to back-reflection of unabsorbed photons into the perovskite layer and therefore to enhanced absorption due to the doubled path length. Integration of the EQE after weighting with the solar spectrum

Table 1. PV Parameters and Efficiency η of Both Subcells, the References, and the Resulting Tandem Efficiency

solar cell	V_{OC} [mV]	J_{SC}[a] [mA/cm^2]	FF [%]	η [%]
perovskite reference cell (Au contact)	1008	20.8	75.2	16.1
perovskite top cell (transparent contact)	1034	16.7	70.3	12.1
CIGS cell (standalone)	689	34.1	78.4	18.4
CIGS bottom cell (tandem configuration)	661	14.4	77.4	7.4
4-terminal tandem cell				19.5

[a]Illumination intensity is 1000 W/m^2 for all cells except for "perovskite reference cell", where it is 984 W/m^2.

DOI: 10.1021/acs.jpclett.5b01108
J. Phys. Chem. Lett. 2015, 6, 2676−2681

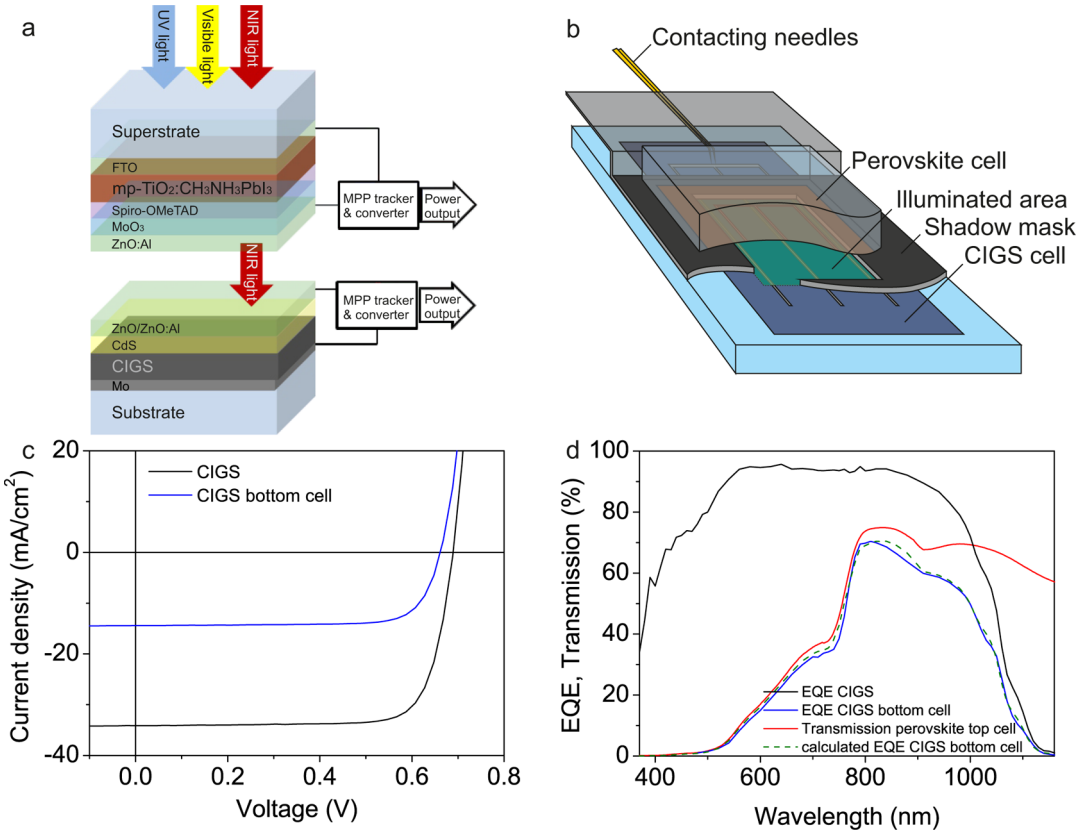

Figure 2. (a) Schematic of a stacked 4-terminal perovskite/CIGS tandem solar cell. The top cell is a perovskite cell in superstrate configuration and the bottom cell is a CIGS cell in substrate configuration. (b) Schematic of the setup for $J-V$ characterization of CIGS bottom solar cells. (c) $J-V$ measurements of a CIGS cell and of the same CIGS cell in a tandem device. The corresponding PV parameters are listed in Table 1. (d) EQE characteristics of a CIGS cell and of the same CIGS cell in a tandem device. Transmission of the perovskite top cell is also shown. Further, the expected bottom cell EQE is shown as obtained by multiplication of the transmission of the perovskite top cell and the EQE of the CIGS cell.

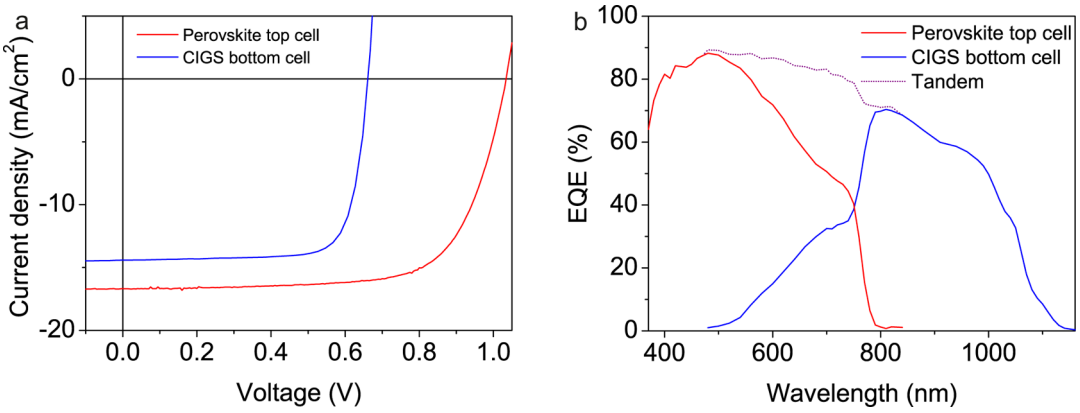

Figure 3. Photovltaic characterization of the best tandem solar cell. (a) $J-V$ measurements of the subcells. The corresponding PV parameters are listed in Table 1. (b) EQE characteristics of the two subcells and their addition (tandem).

leads to an expected J_{SC} of 16.7 mA/cm^2 under AM1.5G, which is in very good agreement with the $J-V$ measurements. Transmission and reflection measurements of the best-performing NIR-transparent perovskite solar cell are shown in Figure 1d. Photons with energy below the band gap are efficiently transmitted with a maximum transmission of 75% at 830 nm and an average transmission of 71% in the wavelength region between 800 and 1000 nm. Reflection measurements reveal an average reflection of 5% in the relevant wavelength region between 350 and 1100 nm. The low reflection is achieved by the application of MgF_2 antireflection (AR) coatings on the glass and ZnO:Al side.

CIGS solar cells are processed with a low temperature coevaporation process[23] and utilized as bottom part in tandem devices. A schematic of the CIGS bottom solar cell and of the complete tandem device are displayed in Figure 2a.

In previous publications on 4-terminal perovskite based tandem solar cells, the performance of the bottom cell was evaluated by reducing the light injection level with gray filters[20] or by calibrating the solar simulator[21] to reach the current expected from EQE measurements. This approach does not

DOI: 10.1021/acs.jpclett.5b01108
J. Phys. Chem. Lett. 2015, 6, 2676−2681

take into account the changed spectrum incident on the bottom cell in the tandem configuration, which can affect the CIGS bottom cell performance.[24] In this work, the CIGS bottom cell performance is measured below a NIR-transparent perovskite solar cell (Figure 2b). A laser-scribed shadow mask with an aperture of 0.213 cm^2 is placed on the CIGS cell, which defines the device area. The mask is extended to above the contacting needles to avoid additional light coupling into the solar cell. The $J-V$ characteristics of a CIGS cell with and without the 12.1% efficient NIR-transparent perovskite top cell are shown in Figure 2c and the corresponding PV parameters are listed in Table 1. Without perovskite top cell, the efficiency of the CIGS solar cell is 18.4%. When adding the NIR-transparent perovskite cell on top of the CIGS solar cell, the FF of the CIGS cell is almost unaffected but the V_{OC} slightly decreases due to the lower illumination intensity. As expected, the J_{SC} is reduced, which is further investigated using EQE measurements (Figure 2d). The expected bottom cell EQE is calculated by multiplication of the EQE of the CIGS cell with the transmission of the perovskite cell. The very good agreement with the measured bottom cell EQE shows that the reduced EQE is fully explained by optical losses in the top cell. Integration of the bottom cell EQE leads to an expected J_{SC} of 14.4 mA/cm^2 under AM1.5G, which is in good agreement with the $J-V$ measurements.

Figure 3a and Table 1 show the $J-V$ characteristics and PV parameters of the two subcells of the described high-performance tandem device.

Such a 4-terminal device can be connected to two separate maximum power point (mpp) trackers (Figure 2a); therefore, the tandem efficiency equals the sum of the efficiencies of the two subcells. With the 4-terminal tandem device presented here, an efficiency of 19.5% has been achieved. This is the highest reported efficiency for polycrystalline tandem solar cells and exceeds the efficiency of both subcells. $J-V$ measurements further reveal that J_{SC} of the two subcells are similar, which is an advantage for future developments of current-matched 2-terminal devices. Figure 3b shows the EQE measurements of the top and bottom cell as well as the tandem EQE as determined by the addition of the two. The tandem EQE is close to 90% in the wavelength region around 500 nm and decreases in the long wavelength region. The reduction is mainly caused by optical losses in three highly conductive TCO layers due to free carrier absorption.

In future devices, we will try to overcome the reduction in FF in the perovskite top cell as compared to the Au reference by utilizing a TCO layer with higher conductivity. To increase the bottom cell efficiency, the transmission of NIR-photons into the CIGS layer should be increased. Reflection at the interface between the two subcells can be reduced by application of an optical coupling layer. Further, parasitic absorption of NIR-light due to free carrier absorption in the TCO layers could be reduced by the utilization of high mobility TCOs like In_2O_3:H, IZO or other emerging materials. Upon these improvements a bottom cell J_{SC} of 17.8 mA/cm^2 can be expected, as calculated using the bottom cell EQE for photons with energy above the perovskite band gap and the EQE of the standalone CIGS cell for lower energy photons. The aforementioned advancements of overcoming resistive and optical losses are expected to lead to tandem devices with efficiency above 22%.

The tandem cell efficiency potential is further estimated using PV characteristics of state-of-the-art perovskite and CIGS solar cells with 20.1% and 21.7% record efficiency.[25,26] The here presented results give confidence, that NIR-transparent perovskite top cells can be produced with V_{OC} and FF as high as the values of opaque cells. Losses in J_{SC} can be overcome by increasing the perovskite layer thickness, allowing this current to be collected in the top cell with reduced thermalization losses. To avoid a reduced V_{OC} and FF due to enhanced recombination in a thicker perovskite, the process might have to be adapted for the use of a larger perovskite thickness.[27,28] The record CIGS cell below the record perovskite cell could reach a J_{SC} of 12 mA/cm^2 as evaluated from EQE measurements,[25,26] assuming negligible optical losses due to absorption in the contact layers (application of high mobility TCOs) and due to reflection at the interface between the two subcells (application of an optical coupling layer). The J_{SC} of 12 mA/cm^2 is slightly lower than in the here presented experimental results due to the comparably small absorber band gap of the perovskite record cell. The results presented here show that it is possible to integrate CIGS solar cells in tandem devices with an essentially unchanged FF and with a V_{OC}, which is reduced by only ~30 mV. According to these considerations, a tandem cell based on state-of-the-art single junction record cells might reach efficiencies above 27% if optical losses can be minimized. Further performance improvements are feasible by enhancing efficiency of the subcells and by shifting the band gap of the bottom cell to a lower value and of the top cell to a higher value.

To conclude, a process for the fabrication of NIR-transparent perovskite solar cells is presented, which enables power conversion efficiencies up to 12.1% and an average transmission of 71% for photons with wavelength between 800 and 1000 nm. The combination of a NIR-transparent perovskite top cell with a CIGS bottom cell enabled a polycrystalline thin film tandem device with 19.5% record efficiency. Future developments of perovskite/CIGS tandem devices are discussed and prospects for devices with further increased efficiency are given.

EXPERIMENTAL SECTION

Solar Cell Preparation. Perovskite solar cells were fabricated on fluorine-doped tin oxide (FTO)-coated glass substrates. Compact TiO_2 was deposited via spray pyrolysis followed by the deposition of a mesoporous TiO_2 layer by spin coating. The perovskite layer was deposited by spin coating and the film was annealed at 90 °C. Doped spiro-OMeTAD[29,30] was subsequently deposited by spin coating. MoO_3 was grown by vacuum evaporation followed by the deposition of ZnO:Al by rf-sputtering. Cell size was defined by mechanical scribing to 0.284 cm^2. MgF_2 AR coatings were applied on both sides of the samples. More details on the perovskite solar cell preparation process can be found in the Supporting Information.

CIGS solar cells were prepared using a process similar to the one previously published.[23] Here, the solar cells were grown on glass substrate with a SiO_2 layer as diffusion barrier for alkaline elements. Molybdenum deposited by DC magnetron sputtering was used as electrical back contact. CIGS was grown using coevaporation at low temperature (~450 °C) in a multistage process with NaF and KF postdeposition treatments.[23] The CdS layer was grown using chemical bath deposition. i-ZnO and ZnO:Al layers were deposited by rf-sputtering and a metallic grid was deposited by electron beam evaporation. A MgF_2 layer is added to reduce reflection losses.

Performance Measurements. $J-V$ characteristics were measured in a sun-simulator under standard AM1.5G spectrum at 1000 W m^{-2} for all measurements except for the perovskite reference

DOI: 10.1021/acs.jpclett.5b01108
J. Phys. Chem. Lett. 2015, 6, 2676−2681

cell with Au contact, which was measured at 984 W m^{-2}. The illumination intensity was calibrated using a c-Si solar cell. Perovskite solar cells were measured from forward bias to short circuit conditions with a step width of 5 mV and 0.5 s settling time at each voltage step (10 mV s^{-1}). The steady-state efficiency was measured by maintaining the cell at constant forward bias and measuring the resulting current. The glass edges of the perovskite solar cell were covered by non-transparent tape. Additional details on the CIGS bottom cell measurements are explained in the main text.

EQE Measurements. EQE measurements were performed using a lock-in amplifier, a chopped white light source, a triple grating monochromator, white light bias, and a c-Si solar cell as reference.

Transmission and Reflection Measurements. Total transmission and reflection spectra were acquired using a UV−vis−NIR spectrophotometer (Shimadzu UV-3600) equipped with an integrating sphere.

Scanning Electron Microscopy (SEM). The microstructure was investigated with a Nova NanoSem230 FEI using 5 kV voltage. The cross section was prepared by mechanical cleaving, and 1 nm of Pt was deposited to avoid charging effects.

■ ASSOCIATED CONTENT

Supporting Information

A detailed description of the perovskite deposition process can be found in the Supporting Information. The Supporting Information is available free of charge on the ACS Publications website at DOI: 10.1021/acs.jpclett.5b01108.

■ AUTHOR INFORMATION

Corresponding Authors

*E-mail: stephan.buecheler@empa.ch. Tel.: +41 (0)58 765 6107. Fax: +41 (0)58 765 1122.

*E-mail: michael.graetzel@epfl.ch. Tel.: +41 (0)21 693 3112. Fax: +41 (0)21 693 6100.

Present Address

⊥(L.K.) ABB Switzerland, Corporate Research, Segelhofstrasse 1K, 5405 Baden Dättwil, Switzerland.

Notes

The authors declare no competing financial interest.

■ ACKNOWLEDGMENTS

Financial support from Swiss National Science Foundation (SNF)-NRP70 (PV2050, 407040-154014, and 407040-153990) as well as from SNF-NanoTera and Swiss Federal Office of Energy (SYNERGY) is gratefully acknowledged. F.F. acknowledges financial support by the Chinese Scholarship Council (CSC). A.A. has received funding from the European Union's Seventh Framework Programme for research, technological development, and demonstration under grant agreement no 291771.

■ REFERENCES

(1) Jean, J.; Brown, P. R.; Jaffe, R. L.; Buonassisi, T.; Bulovic, V. Pathways for Solar Photovoltaics. *Energy Environ. Sci.* **2015**, *8*, 1200−1219.

(2) de Vos, A. Detailed Balance Limit of the Efficiency of Tandem Solar Cells. *J. Phys. D: Appl. Phys.* **1980**, *13*, 839.

(3) NREL Best Research-Cell Efficiencies. http://www.nrel.gov/ncpv/images/efficiency_chart.jpg (accessed May 2015).

(4) Liska, P.; Thampi, K. R.; Grätzel, M.; Bremaud, D.; Rudmann, D.; Upadhyaya, H. M.; Tiwari, A. N. Nanocrystalline Dye-Sensitized Solar Cell/Copper Indium Gallium Selenide Thin-Film Tandem Showing Greater than 15% Conversion Efficiency. *Appl. Phys. Lett.* **2006**, *88*, 203103.

(5) Seyrling, S.; Wenger, S.; Grätzel, M.; Tiwari, A. N. Analysis of Electronic and Optical Losses in Cu(In,Ga)Se_2 /Dye Sensitized Cell Tandem Solar Cells. *Energy Procedia* **2010**, *2*, 199.

(6) You, J.; Dou, L.; Yoshimura, K.; Kato, T.; Ohya, K.; Moriarty, T.; Emery, K.; Chen, C.-C.; Gao, J.; Li, G.; Yang, Y. A Polymer Tandem Solar Cell with 10.6% Power Conversion Efficiency. *Nat. Commun.* **2013**, *4*, 1446.

(7) Wu, X.; Zhou, J.; Duda, A.; Keane, J. C.; Gessert, T. A.; Yan, Y.; Noufi, R. 13·9%-Efficient CdTe Polycrystalline Thin-Film Solar Cells with an Infrared Transmission of ∼50%. *Prog. Photovolt.: Res. Appl.* **2006**, *14*, 471.

(8) Kojima, A.; Teshima, K.; Shirai, Y.; Miyasaka, T. Organometal Halide Perovskites as Visible-Light Sensitizers for Photovoltaic Cells. *J. Am. Chem. Soc.* **2009**, *131*, 6050.

(9) Lee, M. M.; Teuscher, J.; Miyasaka, T.; Murakami, T. N.; Snaith, H. J. Efficient Hybrid Solar Cells Based on Meso-Superstructured Organometal Halide Perovskites. *Science* **2012**, *338*, 643.

(10) Kim, H.-S.; Lee, C.-R.; Im, J.-H.; Lee, K.-B.; Moehl, T.; Marchioro, A.; Moon, S.-J.; Humphry-Baker, R.; Yum, J. H.; Moser, J. E.; et al. Lead Iodide Perovskite Sensitized All-Solid-State Submicron Thin Film Mesoscopic Solar Cell with Efficiency Exceeding 9%. *Sci. Rep* **2012**, *2*, 591.

(11) Burschka, J.; Pellet, N.; Moon, S.-J.; Humphry-Baker, R.; Gao, P.; Nazeeruddin, M. K.; Grätzel, M. Sequential Deposition as a Route to High-Performance Perovskite-Sensitized Solar Cells. *Nature* **2013**, *499*, 316.

(12) Liu, M.; Johnston, M. B.; Snaith, H. J. Efficient Planar Heterojunction Perovskite Solar Cells by Vapour Deposition. *Nature* **2013**, *501*, 395.

(13) Jeon, N. J.; Noh, J. H.; Yang, W. S.; Kim, Y. C.; Ryu, S.; Seo, J.; Il Seok, S. Compositional Engineering of Perovskite Materials for High-Performance Solar Cells. *Nature* **2015**, *476*, 517.

(14) de Wolf, S.; Holovsky, J.; Moon, S.-J.; Löper, P.; Niesen, B.; Ledinsky, M.; Haug, F.-J.; Yum, J.-H.; Ballif, C. Organometallic Halide Perovskites: Sharp Optical Absorption Edge and Its Relation to Photovoltaic Performance. *J. Phys. Chem. Lett.* **2014**, *5*, 1035.

(15) Noh, J. H.; Im, S. H.; Heo, J. H.; Mandal, T. N.; Il Seok, S. Chemical Management for Colorful, Efficient, and Stable Inorganic−Organic Hybrid Nanostructured Solar Cells. *Nano Lett.* **2013**, *13*, 1764.

(16) Snaith, H. J. Perovskites: The Emergence of a New Era for Low-Cost, High-Efficiency Solar Cells. *J. Phys. Chem. Lett.* **2013**, *4*, 3623.

(17) Kranz, L.; Jäger, T.; Reinhard, P.; Hagendorfer, H.; Romanyuk, Y. E.; Buecheler, S.; Tiwari, A. N. Trihalide Perovskite Planar Heterojunction Solar Cells Combined with Cu(In,Ga)Se_2 Devices in Tandem Structures. *2013 MRS Fall Meeting & Exhibit.*

(18) Gao, P.; Grätzel, M.; Nazeeruddin, M. K. Organohalide Lead Perovskites for Photovoltaic Applications. *Energy. Environ. Sci.* **2014**, *7*, 2448.

(19) Todorov, T.; Gershon, T.; Gunawan, O.; Sturdevant, C.; Guha, S. Perovskite-Kesterite Monolithic Tandem Solar Cells with High Open-Circuit Voltage. *Appl. Phys. Lett.* **2014**, *105*, 173902.

(20) Löper, P.; Moon, S.-J.; Martin de Nicolas, S.; Niesen, B.; Ledinsky, M.; Nicolay, S.; Bailat, J.; Yum, J. H.; de Wolf, S.; Ballif, C. Organic−Inorganic Halide Perovskite/Crystalline Silicon Four-Terminal Tandem Solar Cells. *Phys. Chem. Chem. Phys.* **2015**, *17*, 1619.

(21) Bailie, C. D.; Christoforo, M. G.; Mailoa, J. P.; Bowring, A. R.; Unger, E. L.; Nguyen, W. H.; Burschka, J.; Pellet, N.; Lee, J. Z.; Grätzel, M.; et al. Semi-Transparent Perovskite Solar Cells for Tandems with Silicon and CIGS. *Energy Environ. Sci.* **2015**, *8*, 956.

(22) Snaith, H. J.; Abate, A.; Ball, J. M.; Eperon, G. E.; Leijtens, T.; Noel, N. K.; Stranks, S. D.; Wang, J. T.-W.; Wojciechowski, K.; Zhang, W. Anomalous Hysteresis in Perovskite Solar Cells. *J. Phys. Chem. Lett.* **2014**, *5*, 1511.

(23) Chirila, A.; Reinhard, P.; Pianezzi, F.; Bloesch, P.; Uhl, A. R.; Fella, C.; Kranz, L.; Keller, D.; Gretener, C.; Hagendorfer, H.; et al.

DOI: 10.1021/acs.jpclett.5b01108
J. Phys. Chem. Lett. 2015, 6, 2676−2681

Potassium-Induced Surface Modification of Cu(In,Ga)Se_2 Thin Films for High-Efficiency Solar Cells. *Nat. Mater.* **2013**, *12*, 1107.
(24) Igalson, M.; Urbaniak, A.; Zabierowski, P.; Abdel Maksoud, H.; Buffiere, M.; Barreau, N.; Spiering, S. Red-Blue Effect in Cu(In,Ga)-Se_2-Based Devices Revisited. *Thin Solid Films* **2013**, *535*, 302.
(25) Seok Yang, W.; Hong Noh, J.; Joong Jeon, N.; Chan Kim, Y.; Ryu, S.; Seo, J.; Il Seok, S. High-Performance Photovoltaic Perovskite Layers Fabricated through Intramolecular Exchange. *Science* **2015**, *348*, 1234.
(26) Jackson, P.; Hariskos, D.; Wuerz, R.; Kiowski, O.; Bauer, A.; Friedlmeier, T. M.; Powalla, M. Properties of Cu(In,Ga)Se_2 Solar Cells with New Record Efficiencies up to 21.7%. *Phys. Stat. Sol. RRL* **2015**, *9*, 28.
(27) Xiao, Z.; Dong, Q.; Bi, C.; Shao, Y.; Yuan, Y.; Huang, J. Solvent Annealing of Perovskite-Induced Crystal Growth for Photovoltaic-Device Efficiency Enhancement. *Adv. Mater.* **2014**, *26*, 6503.
(28) Momblona, C.; Malinkiewicz, O.; Roldán-Carmona, C.; Soriano, A.; Gil-Escrig, L.; Bandiello, E.; Scheepers, M.; Edri, E.; Bolink, H. J. Efficient Methylammonium Lead Iodide Perovskite Solar Cells with Active Layers from 300 to 900 nm. *APL Mater.* **2014**, *2* (8), 081504.
(29) Abate, A.; Leijtens, T.; Pathak, S.; Teuscher, J.; Avolio, R.; Errico, M. E.; Kirkpatrik, J.; Ball, J. M.; Docampo, P.; McPherson, I.; Snaith, H. J. Lithium Salts as "Redox Active" p-Type Dopants for Organic Semiconductors and Their Impact in Solid-State Dye-Sensitized Solar Cells. *Phys. Chem. Chem. Phys.* **2013**, *15*, 2572.
(30) Burschka, J.; Dualeh, A.; Kessler, F.; Baranoff, E.; Cevey-Ha, N. L.; Yi, C.; Nazeeruddin, M. K.; Grätzel, M. Tris(2-(1*H*-pyrazol-1-yl)pyridine)cobalt(III) as p-Type Dopant for Organic Semiconductors and Its Application in Highly Efficient Solid-State Dye-Sensitized Solar Cells. *J. Am. Chem. Soc.* **2011**, *133*, 18042.

DOI: 10.1021/acs.jpclett.5b01108
J. Phys. Chem. Lett. 2015, 6, 2676−2681